Ibn Al-Haitham Journal for Pure and Applied Sciences
Journal homepage: jih.uobaghdad.edu.iq
PISSN: 1609-4042, EISSN: 2521-3407
IHJPAS. 2025, 38 (1)

Effect of Couple-Stress on Peristaltic Transport of Sutterby Fluid in an Asymmetric Channel

Asmaa A. Mohammed [1*] and Liqaa Zeki Hummady [2]
[1] Department of Mathematics, College of Science, University of Baghdad, Baghdad, Iraq.
[1,2] Department of Mathematics, College of Science for Women, University of Baghdad, Baghdad, Iraq.
*Corresponding Author.

Received:6 May 2023 Accepted: 14 August 2023 Published:20 January 2025
doi.org/10.30526/38.1.3462

Abstract

In this paper, the effect of a couple–stress and other variables on the peristaltic flow of Sutterby fluid in an inclined asymmetric channel containing a porous medium with heat transfer is examined. In the presence of rotation and couple–stress, mathematical modeling is developed using constitutive equations based on the model of Sutterby fluid. In flow analysis, assumptions such as long wavelength approximation and low Reynolds number are used. The resulting nonlinear equation was numerically solved using the perturbation method. The effects of various physical parameters such as the couple-stress parameter, the Grashof number, the Hartmann number, the Reynold number, the Froude number, the Hall parameter, the Darcy number, the magnetic field, the Sutterby fluid parameter, and heat transfer analysis on the stream function are analyzed graphically. Utilizing MATHEMATICA software, numerical results were computed.

Keywords: Peristaltic flow, Heat transform, Inclined channel, Porous medium, Couple-stress, and Sutterby fluid.

1. Introduction

Peristaltic pumping is a special type of pumping when it is simple to transport a variety of complex rheological fluids from one location to another. This pumping principle is referred to as peristaltic (1). Some examples of such physiological processes are the passage of food, chyme, and urine. Peristalsis is the driving force behind everything from worm movement to the transfer of noxious and clean fluids to the operation of finger pumps and the heart-lung machine. Damping, dispensability, and tension in the vasculature play a critical part in physiological processes involving peristalsis, such as blood flow (2). Studies of peristalsis were first introduced by (3,4). Since then, researchers have made numerous attempts to dissect the peristaltic movement of fluids and its implications in the medical and business worlds. In biological systems and industrial fluid transport, heat transfer is a fundamental principle. One of the most essential roles of the cardiovascular system is maintaining the body's temperature. Air that enters the lungs must also be tempered to the body's temperature. This is accomplished through the use of all blood vessels. There are three methods of heat transmission; however, convection is the most relevant for fluid circulation in the human body. Human and animal bodies use convection heat transfer to release heat generated by metabolic processes into the environment (1). In recent years, the effects of changing viscosity, heat transfer, and mass transfer on magnetohydrodynamic (MHD) peristaltic flow in an asymmetric tapering inclined channel with porous material were Examined (5). For a high magnetic field like in MHD flows, hall current has significant effects. This phenomenon is widely used in a variety of fields, including the design of power generators, Hall accelerators, refrigeration coils, electric transformers, and spacecraft propulsion systems. The peristaltic transport in the presence of Hall current has been the subject of several published works. The effect of Hall current, viscosity variation, and porous medium on the peristaltic transport of viscoelastic fluid through irregular microchannels was studied (6). The effect of magnetohydrodynamic (MHD) on a viscous fluid generalized burgers' fluid with a gradient constant pressure and an exponentially accelerating plate, where the no-slip hypothesis between the burgers' fluid and the exponential plate is no longer applicable, were studied (7). (8) studied a couple stress of peristaltic transport of Sutterby micropolar nanofluid within a symmetric channel with a powerful magnetic field and Hall currents effect. The influence of couple stress as well as rotation on the peristaltic flow of a Powell-Eyring in an inclined, tapered, and asymmetrical channel investigates by (9). (10) have examined the effect of MHD on a peristaltic flow of Newtonian fluid with a couple stress through porous media, where the assumption of no slippage between the wall and the fluid is no longer applicable.

Since (11–13) examined the mechanism of peristaltic transport, it has attracted the interest of numerous researchers. Viscous liquids are less prevalent in industrial and physiological processes than non-Newtonian fluids. Shampoo, ketchup, lubricants, paints, and blood are all examples of non-Newtonian substances found in nature. Among that, Sutterby liquid (14) is one of the materials that characterize ionic high polymer solutions. Convection and Hall current was used to simulate the MHD peristaltic transport of a Sutterby nanofluid (15). Waveform motion of non-Newtonian fluids through porous channels is discussed (16,17), where the effects of rotation and an inclined MHD are considered. Magnetohydrodynamic (MHD) for Williamson fluid with variable temperatures and variable concentrations in a slanted channel with variable viscosity has been investigated (18). The effects of radiation and convection in a Sutterby fluid are discussed (19). In Ramesh (20), electroosmotic peristaltic transport of Sutterby nanofluids is investigated. The peristaltic flow of a Sutterby liquid in an inclined channel was investigated (21).

In this paper, the study will look at the effects of rotation on heat transfer for peristaltic transport in an inclined asymmetric channel with a porous medium. This will be done by using different values of the parameters of rotation, amplitude wave, and channel taper, as well as different values of the Grashof number, the Hartmann number, the Reynold number, the Froude number, the Hall parameter, the Darcy number, the magnetic field, the Sutterby fluid parameter, and heat transfer analysis, based on the changes in stream function.

2. Materials and Methods

2.1. A mathematical formulation for asymmetric flow

Consider the peristaltic transport of an incompressible Sutterby fluid through a two-dimensional asymmetric conduit that has a width of $(d' + d)$. whereas motion is constant within a coordinate system pumped at wave speed (c) in the wave framer $(\bar{X}, \bar{Y})$.

The geometry of a wall's structure is described as:

$$\overline{h_1}(\bar{X},\bar{t}) = d - a_1 \sin\left[\frac{2\pi}{\lambda}(\bar{x} - c\bar{t})\right] \quad (1)$$

$$\overline{h_2}(\bar{X},\bar{t}) = -d' - a_2 \sin\left[\frac{2\pi}{\lambda}(\bar{x} - c\bar{t}) + \Phi\right] \quad (2)$$

In which $\overline{h_1}(\bar{X},\bar{t})$, $\overline{h_2}(\bar{X},\bar{t})$ are the lower and upper wall respectively, (d, d') indicates the channel width, (a_1, a_2) are the wave's amplitudes, (λ) represents the wavelength, (c) is the speed of a wave, (Φ) varies in the range $(0 \leq \Phi \leq \pi)$, when the value of $\Phi = 0$ the channel is symmetric with waves out of phase and $\Phi = \pi$ waves are in phase the rectangular coordinates has been designed in such a method that $\bar{X} - axis$ is along the path that waves use for propagation and $\bar{Y} - axis$ perpendicular to $\bar{X}, \bar{t}$ represents the time.

Further a_1, a_2, d, d' and Φ satisfy the following condition

$$a_1^2 + a_2^2 + 2\mathrm{a}_1\mathrm{a}_2 \cos\Phi \leq (d + d')^2 \quad (3)$$

2.2 Basic equation

The additional stress tensor for the Sutterby model is determined by (20):

$$\bar{\mathrm{S}} = \frac{\mu}{2}\left[\frac{\sinh^{-1}(\mathrm{n}\dot{\gamma})}{\mathrm{n}\dot{\gamma}}\right]^{m^*} \mathrm{A}_1 \quad (4)$$

$$\dot{\gamma} = \sqrt{\frac{1}{2}\mathrm{tras}(\mathrm{A}_1)^2} \quad (5)$$

$$\mathrm{A}_1 = \nabla\bar{\mathrm{V}} + (\nabla\bar{\mathrm{V}})^{\mathrm{T}} \quad (6)$$

Where $\bar{S}$ denotes the stress of the extra tensor, n, and m^* represents the material constants of the Sutterby fluid, $\nabla = (\partial\bar{X}, \partial\bar{Y}, 0)$ is the gradient vector, μ represents the dynamic viscosity and A_1 represents the first Rivilin–Ericksen tensor. The phrase $\sinh^{-1}$ is approximately equivalent to

$$\sinh^{-1}\left(\frac{\dot{\gamma}}{n}\right) = \frac{\dot{\gamma}}{\mathrm{n}} - \frac{\dot{\gamma}^3}{6\mathrm{n}^3} \quad , \left|\frac{\dot{\gamma}^5}{6\mathrm{n}^5}\right| \ll 1 \quad (7)$$

The constituents of the extra stress tensor of Sutterby defined by Equation ((4) are listed below:

$$\bar{S}_{\bar{X}\bar{X}} = \frac{\mu}{2}[1 - \frac{mn^2}{6}\left(2\bar{U}_{\bar{X}}{}^2 + (\bar{V}_{\bar{X}} + \bar{U}_{\bar{Y}})^2 + 2\bar{V}_{Y}{}^2\right)]2\bar{U}_{\bar{X}} \quad (8)$$

$$\bar{S}_{\bar{X}\bar{Y}} = \frac{\mu}{2}\left[1 - \frac{mn^2}{6}\left(2\bar{U}_{\bar{X}}{}^2 + (\bar{V}_{\bar{X}} + \bar{U}_{\bar{Y}})^2 + 2\bar{V}_{Y}{}^2\right)\right](\bar{U}_{\bar{X}} + \bar{V}_{\bar{Y}}) \quad (9)$$

$$\bar{S}_{\bar{Y}\bar{Y}} = \frac{\mu}{2}\left[1 - \frac{mn^2}{6}\left(2\bar{U}_{\bar{X}}{}^2 + (\bar{V}_{\bar{X}} + \bar{U}_{\bar{Y}})^2 + 2\bar{V}_{Y}{}^2\right)\right]2\bar{V}_{\bar{Y}} \quad (10)$$

2.3. The governing equations

The flow is controlled by three coupled nonlinear partial differentials of continuity, momentum, and energy, the governing equations in frame $(\bar{X}, \bar{Y})$ can be written as follows:

$$\frac{\partial\bar{U}}{\partial\bar{X}} + \frac{\partial\bar{V}}{\partial\bar{Y}} = 0 \quad (11)$$

$$\rho\left(\frac{\partial\bar{U}}{\partial\bar{t}} + \bar{U}\frac{\partial\bar{U}}{\partial\bar{X}} + \bar{V}\frac{\partial\bar{U}}{\partial\bar{Y}}\right) - \rho\Omega\left(\Omega\bar{U} + 2\frac{\partial\bar{V}}{\partial\bar{t}}\right) = -\frac{\partial\bar{P}}{\partial\bar{X}} + \frac{\partial\bar{S}_{\bar{X}\bar{X}}}{\partial\bar{X}} + \frac{\partial\bar{S}_{\bar{X}\bar{Y}}}{\partial\bar{Y}} - \frac{\sigma B_0{}^2}{(1+m^2)}(\bar{U} - m\bar{V}) + \mathrm{g}\rho\beta_T(T - T_0) - \frac{\mu}{k_0}\bar{U} - \mu_1\nabla^4\bar{U} + \rho g sin(\alpha 1) \quad (12)$$

$$\rho\left(\frac{\partial\bar{V}}{\partial\bar{t}} + \bar{U}\frac{\partial\bar{V}}{\partial\bar{X}} + \bar{V}\frac{\partial\bar{V}}{\partial\bar{Y}}\right) - \rho\Omega\left(\Omega\bar{V} - 2\frac{\partial\bar{U}}{\partial\bar{t}}\right) = -\frac{\partial\bar{P}}{\partial\bar{Y}} + \frac{\partial\bar{S}_{\bar{X}\bar{Y}}}{\partial\bar{X}} + \frac{\partial\bar{S}_{\bar{Y}\bar{Y}}}{\partial\bar{Y}} - \frac{\sigma B_0{}^2}{(1+m^2)}(\bar{V} + m\bar{U}) - \frac{\mu}{k_0}\bar{V} - \mu_1\nabla^4\bar{V} + \rho g cos(\alpha 1) \quad (13)$$

$$\rho C_P\left(\frac{\partial}{\partial\bar{t}} + \bar{U}\frac{\partial}{\partial\bar{X}} + \bar{V}\frac{\partial}{\partial\bar{Y}}\right)\bar{T} = \kappa\left(\frac{\partial^2}{\partial\bar{t}^2} + \frac{\partial^2}{\partial\bar{X}^2} + \frac{\partial^2}{\partial\bar{Y}^2}\right)\bar{T} + \varphi_0 \quad (14)$$

Where ρ is the fluid density, $(\bar{U}, \bar{V})$ the velocity components, $\bar{P}$ represents the hydrodynamic pressure, $\bar{S}_{\bar{X}\bar{X}}, \bar{S}_{\bar{X}\bar{Y}}$, and $\bar{S}_{\bar{Y}\bar{Y}}$ are the constituents of the extra stress tensor $\bar{S}$. σ is the electrical conductivity, φ_0 is the steady heat addition/absorption, B_0 is an applied magnetic field, β_T is the thermal expansion coefficient, g is the gravitational acceleration, μ_1 is a constant link to the couple stress, and Ω represents the rotation. The specific heat is denoted by C_P, $\alpha 1$ is the channel's angle of an inclination concerning the horizontal axis, k_0 material constant, the thermal conductivity by k, and the temperature by $\bar{T}$. And

$$\nabla^2 = \frac{\partial^2}{\partial \bar{X}^2} + \frac{\partial^2}{\partial \bar{Y}^2}, \nabla^4 = \frac{\partial^4}{\partial \bar{X}^4} + 2\frac{\partial^4}{\partial \bar{X}^2 \partial \bar{Y}^2} + \frac{\partial^4}{\partial \bar{Y}^4}$$

Peristaltic movement in reality is an unsteady behavior, but it can be considered to be steady via the change from the experimental frame (fixed frame) $(\bar{X}, \bar{Y})$ to the wave frame (move frame) $(\bar{x}, \bar{y})$. The following transformations establish the link between coordinates, velocities, and pressure in laboratory frame $(\bar{X}, \bar{Y})$ to wave frame $(\bar{x}, \bar{y})$:

$$\bar{X} = \bar{x} - c\bar{t} \ , \bar{Y} = \bar{y} \ , \bar{U} = \bar{u} - c \ , \bar{V} = \bar{v} \ , \bar{P}(\bar{X}, \bar{Y}, \bar{t}) = \bar{p}(\bar{x}, \bar{y}) \tag{15}$$

Where $\bar{u}$ and $\bar{v}$ represent the components of velocity, and $\bar{p}$ denotes the pressure in the wave frame. Now, Equations (15) will be substituted into Equations (1),(2) and (8)-(14) and then normalize the equation that is produced by doing so by utilizing the non-dimensional quantities that are listed as follows:

$$x = \frac{1}{\lambda}\bar{x}, y = \frac{1}{d}\bar{y}, u = \frac{1}{c}\bar{u}, v = \frac{1}{c}\bar{v}, a = \frac{a1}{d}, b = \frac{a2}{d}, d1 = \frac{d'}{d}, p = \frac{d^2}{\lambda \mu c}\bar{p}, t = \frac{c}{\lambda}\bar{t}, h_1 = \frac{1}{d}\overline{h_1}, h_2 = \frac{1}{d}\overline{h_2}, \delta = \frac{d}{\lambda}, Re = \frac{\rho c d}{\mu}, \bar{T} = T - T_0, \theta = \frac{T - T_0}{T_1 - T_0}, S_{ij} = \frac{d}{\mu c}\bar{S}_{\bar{I}\bar{J}}, Gr = \frac{g\beta_T(T - T_0)d^2}{\mu c}, Pr = \frac{\mu c_p}{k}, Fr = \frac{c^2}{gd}, Da = \frac{k_0}{d^2}, \alpha = d\sqrt{\frac{\mu}{\mu_1}} \tag{16}$$

Where, (δ) represents the wave number, (h_1) *and* (h_2) is the nondimensional upper and lower wall surface respectively, (*Re*) represents the Reynolds number, (*Pr*) represents the Prandtl number, (*Gr*) represents the Grashof number, (*Fr*) represents the Froude number, (*M*) represents the Hartman number, (*Da*) represents Darcy number, (Φ) represents the face difference,(A) represents the parameter of Sutterby liquid, (α) represents the couple stress parameter, and (T_0) *and* (T_1) are the wall temperatures at the top and bottom, respectively. Then, in view of Equations (16), (1), (2), and (8)-(14) take the form :

$$h_1(x) = 1 + a \sin x \tag{17}$$

$$h_2(x) = -d_1 - b \sin(x + \Phi) \tag{18}$$

$$\delta\frac{\partial u}{\partial x} + \frac{\partial v}{\partial y} = 0 \tag{19}$$

$$Re\left(\delta\frac{\partial u}{\partial t} + \delta u\frac{\partial u}{\partial x} + v\frac{\partial u}{\partial y}\right) - \frac{\rho d^2}{\mu}\Omega\left(\Omega u + 2\delta\frac{\partial v}{\partial t}\right) = -\frac{\partial p}{\partial x} + \delta\frac{\partial S_{xx}}{\partial x} + \frac{\partial S_{xy}}{\partial y} - \frac{\sigma B_0{}^2}{(1+m^2)}(u - mv) + Gr\,\theta - \frac{1}{Da}u - \frac{1}{\alpha^2}\left(\delta^4\frac{\partial^4 u}{\partial x^4} + 2\delta^2\frac{\partial^4 u}{\partial x^2 \partial y^2} + \frac{\partial^4 u}{\partial y^4}\right) + \frac{Re}{Fr}\sin(\alpha 1) \tag{20}$$

$$Re\delta\left(\delta\frac{\partial v}{\partial t} + \delta u\frac{\partial v}{\partial x} + v\frac{\partial v}{\partial y}\right) - Re\frac{d}{c}\Omega\left(\Omega\delta v - 2\delta^2\frac{\partial u}{\partial t}\right) = -\frac{\partial p}{\partial y} + \delta^2\frac{\partial S_{xy}}{\partial x} + \delta\frac{\partial S_{yy}}{\partial y} - \frac{\sigma B_0{}^2}{(1+m^2)}\frac{d^2}{\mu}\delta(v + mu) - \frac{1}{Da}\delta v - \frac{1}{\alpha^2}\left(\delta^5\frac{\partial^4 v}{\partial x^4} + 2\delta^3\frac{\partial^4 v}{\partial x^2 \partial y^2} + \delta\frac{\partial^4 v}{\partial y^4}\right) + \frac{Re}{Fr}\cos(\alpha 1) \tag{21}$$

$$RePr\delta\left(\frac{\partial}{\partial t} + u\frac{\partial}{\partial x} + v\frac{\partial}{\partial y}\right)\theta = \left(\delta^2\frac{c^2\partial^2}{\partial t^2} + \delta^2\frac{\partial^2}{\partial x^2} + \frac{\partial^2}{\partial y^2}\right)\theta + B \tag{22}$$

Introduction to fluid flow (ψ) through a relationship:

$$u = \psi_y \, , v = -\delta \psi_x \tag{23}$$

Substituted Equations (23) into Equations (19)-(22) respectively,

$$\delta \frac{\partial \psi_y}{\partial x} - \delta \frac{\partial \psi_x}{\partial y} = 0 \tag{24}$$

$$Re\left(\delta \frac{\partial \psi_y}{\partial t} + \delta \psi_y \frac{\partial \psi_y}{\partial x} - \delta \psi_x \frac{\partial \psi_y}{\partial y}\right) - \frac{\rho \mathrm{d}^2}{\mu} \Omega \left(\Omega \psi_y - 2\delta^2 \frac{\partial \psi_x}{\partial t}\right) = -\frac{\partial p}{\partial x} + \delta \frac{\partial S_{xx}}{\partial x} + \frac{\partial S_{xy}}{\partial y} - \frac{\sigma {B_0}^2}{(1+m^2)}\left(\psi_y + m\delta\psi_x\right) + \mathrm{Gr}\,\theta - \frac{1}{Da}\psi_y - \frac{1}{\alpha^2}\left(\delta^4 \frac{\partial^4 \psi_y}{\partial x^4} + 2\delta^2 \frac{\partial^4 \psi_y}{\partial x^2 \partial y^2} + \frac{\partial^4 \psi_y}{\partial y^4}\right) + \frac{Re}{Fr}\sin(\alpha 1) \tag{25}$$

$$Re\delta\left(-\delta^2 \frac{\partial \psi_x}{\partial t} - \delta^2 \psi_y \frac{\partial \psi_x}{\partial x} - \delta^2 \psi_x \frac{\partial \psi_x}{\partial y}\right) - Re \frac{d}{c} \Omega \left(-\Omega \delta^2 \psi_x - 2\delta^2 \frac{\partial \psi_y}{\partial t}\right) = -\frac{\partial p}{\partial y} + \delta^2 \frac{\partial S_{xy}}{\partial x} + \delta \frac{\partial S_{yy}}{\partial y} + \frac{\sigma {B_0}^2}{(1+m^2)} \frac{d^2}{\mu} \delta\left(-\delta \psi_x + m\psi_y\right) + \frac{1}{Da}\delta\psi_x - \frac{1}{\alpha^2}(-\delta^6 \frac{\partial^4 \psi_x}{\partial x^4} - 2\delta^4 \frac{\partial^4 \psi_x}{\partial x^2 \partial y^2} - \delta^2 \frac{\partial^4 \psi_x}{\partial y^4}) + \frac{Re}{Fr}\cos(\alpha 1) \tag{26}$$

$$RePr\delta\left(\frac{\partial}{\partial t} + \psi_y \frac{\partial}{\partial x} - \delta \psi_x \frac{\partial}{\partial y}\right)\theta = \left(\delta^2 \frac{c^2 \partial^2}{\partial t^2} + \delta^2 \frac{\partial^2}{\partial x^2} + \frac{\partial^2}{\partial y^2}\right)\theta + B \tag{27}$$

When (δ <<1), the Equations (25)-(27) become as follows:

$$-\frac{\rho \mathrm{d}^2}{\mu} \Omega^2 \psi_y = -\frac{\partial p}{\partial x} + \frac{\partial S_{xy}}{\partial y} - \left(\frac{M^2}{1+m^2} + \frac{1}{Da}\right)\psi_y + Gr\,\theta - \frac{1}{\alpha^2}\frac{\partial^5 \psi}{\partial y^5} + \frac{Re}{Fr}\sin(\alpha 1) \tag{28}$$

$$-\frac{\partial p}{\partial y} = 0 \tag{29}$$

$$\frac{\partial^2 \theta}{\partial y^2} + \mathrm{B} = 0 \tag{30}$$

While an additional stress tensor component takes the following form:

$$s_{xy} = \frac{1}{2}\frac{\partial^2 \psi}{\partial y^2} - A\left(\frac{\partial^2 \psi}{\partial y^2}\right)^3, s_{xx} = 0, s_{yy} = 0 \tag{31}$$

Where $M = \sqrt{\frac{\sigma}{\mu}} B_0 d$ the Hartman number, $A = \boldsymbol{\frac{mb^2c^2}{6d^2}}$ the Sutterby liquid parameter and $B = \frac{d^2 \varphi_0}{k(T_1 - T_0)}$ the constant heat radiation

If Equation (31) is substituted into Equation (28) and the derivative concerning y is taken, the following equation is obtained

$$:\frac{2}{\alpha^2}\frac{\partial^6 \psi}{\partial y^6} - \frac{\partial^4 \psi}{\partial y^4}\left[1 - 3A\left(\frac{\partial^2 \psi}{\partial y^2}\right)^2\right] + 6A\frac{\partial^2 \psi}{\partial y^2}\left(\frac{\partial^3 \psi}{\partial y^3}\right)^2 - 2\left(\frac{\rho \mathrm{d}^2}{\mu}\Omega^2 - \frac{M^2}{m^2+1} - \frac{1}{Da}\right)\frac{\partial^2 \psi}{\partial y^2} - 2Gr\frac{\partial \theta}{\partial y} = 0 \tag{32}$$

$$\frac{\partial^2 \theta}{\partial y^2} + B = 0 \tag{33}$$

In wave frames, the dimensionless boundary conditions are:

$$\frac{\partial\psi}{\partial y}+\beta\frac{\partial^2\psi}{\partial y^2}=-1, \psi=\frac{F}{2}, \frac{\partial^3\psi}{\partial y^3}=0 \quad at\ y=h_1 \tag{34}$$

$$\frac{\partial\psi}{\partial y}-\beta\frac{\partial^2\psi}{\partial y^2}=-1, \psi=-\frac{F}{2}, \frac{\partial^3\psi}{\partial y^3}=0 \quad at\ y=h_2 \tag{35}$$

$$\theta=0\ \ at\ y=h_1\ , \theta=1\ \ at\ y=h_2 \tag{36}$$

Where F is just the flow rate, which is dimensionless in time in the frame of the wave. It is associated with the form that has no dimensions' temporal flow rate *Q1* in the experimental frame via the expression:

$$Q_1=F+1+d \tag{37}$$

as a, b, Φ, and d achieve Equation (3):

$$a^2+b^2+2abcos(\Phi)\le(1+d_1)^2 \tag{38}$$

Initially, the nonlinear equation Equation (33) is solved by integrating and substituting the boundary conditions Equation (36), and then the solution to Equation (37) is obtained :

$$\theta=-\frac{-2\mathrm{h}_1+\mathrm{h}_1^2\mathrm{h}_2B-\mathrm{h}_1\mathrm{h}_2^2B}{2(h_1-\mathrm{h}_2)}-\frac{(2-\mathrm{h}_1^2B+\mathrm{h}_2^2B)y}{2(\mathrm{h}_1-\mathrm{h}_2)}-\frac{By^2}{2} \tag{39}$$

By differentiating Equation (39) to y and substituting it into Equation (32), obtaining the following nonlinear equation:

$$\frac{2}{\alpha^2}\frac{\partial^6\psi}{\partial y^6}-\frac{\partial^4\psi}{\partial y^4}\left[1-3A\left(\frac{\partial^2\psi}{\partial y^2}\right)^2\right]+6A\frac{\partial^2\psi}{\partial y^2}\left(\frac{\partial^3\psi}{\partial y^3}\right)^2-2\left(\frac{\rho\mathrm{d}^2}{\mu}\Omega^2-\frac{M^2}{m^2+1}-\frac{1}{Da}\right)\frac{\partial^2\psi}{\partial y^2}+ \\ 2Gr\left(-\frac{(2-\mathrm{h}_1^2B+\mathrm{h}_2^2B)}{2(\mathrm{h}_1-\mathrm{h}_2)}-\ \mathrm{By}\right)=0 \tag{40}$$

2.4. Solution of the problem

It is not possible to that construct a solution in closed form for every one of the arbitrary parameters involved in Equation (40), as it is highly non-linear and convoluted. Therefore, the perturbation approach is used to get the answer. The solution was expanded to include perturbation (22) :

$$\psi=\psi_0+A\psi_1+o(A^2) \tag{41}$$

And by substituting the expressions Equation (41) into Equation (40), along with the boundary conditions Equation (34) and Equation (35) and equating the coefficients of similar powers of A, The following system of equations is obtained:

2.4.1. Zeroth order system

When such terms of order (A) in a zero-order system are negligible, the result is

$$\frac{2}{\alpha^2}\frac{\partial^6\psi_0}{\partial \mathrm{y}^6}-\frac{\partial^4\psi_0}{\partial \mathrm{y}^4}-\zeta\frac{\partial^2\psi_0}{\partial \mathrm{y}^2}+\gamma y-\eta=0 \tag{42}$$

Where $\zeta=2(\frac{\rho d^2}{\mu}\Omega^2-\frac{1}{Da}-\frac{M^2}{m^2+1})$, $\gamma=2GrB$, and $\eta=Gr[B(h_1+h_2)-\frac{2}{h_1-h_2}]$

Such that

$$\frac{\partial\psi_0}{\partial y}+\beta_1\frac{\partial^2\psi_0}{\partial y^2}=-1,\psi_0=\frac{F_0}{2},\frac{\partial^3\psi_0}{\partial y^3}=0 \quad at\ y=h_1 \tag{43}$$

and

$$\frac{\partial\psi_0}{\partial y}-\beta_1\frac{\partial^2\psi_0}{\partial y^2}=-1,\psi_0=-\frac{F_0}{2},\frac{\partial^3\psi_0}{\partial y^3}=0 \quad at\ y=h_2 \tag{44}$$

2.4.2. First order system

$$\frac{2}{\alpha^2}\ \frac{\partial^6\psi_1}{\partial y^6}-\frac{\partial^4\psi_1}{\partial y^4}-\zeta\frac{\partial^2\psi_1}{\partial y^2}+3\frac{\partial^4\psi_0}{\partial y^4}\left(\frac{\partial^2\psi_0}{\partial y^2}\right)^2+6\frac{\partial^2\psi_0}{\partial y^2}\left(\frac{\partial^3\psi_0}{\partial y^3}\right)^2+\gamma y-\eta=0 \tag{45}$$

$$\frac{\partial\psi_1}{\partial y}+\beta_1\frac{\partial^2\psi_1}{\partial y^2}=-1,\psi_1=\frac{F_1}{2},\frac{\partial^3\psi_1}{\partial y^3}=0 \quad at\ y=h_1 \tag{46}$$

and

$$\frac{\partial\psi_1}{\partial y}-\beta_1\frac{\partial^2\psi_1}{\partial y^2}=-1,\psi_1=-\frac{F_1}{2},\frac{\partial^3\psi_1}{\partial y^3}=0 \quad at\ y=h_2 \tag{47}$$

Solving the relevant zeroth-order and first-order systems yields the final stream function equation.

$$\psi=\psi_0+\mathrm{A}\psi_1 \tag{48}$$

3. Results

This section consists of one subsection. Using MATHEMATICA, the velocity distribution is depicted in the first, and the pressure gradient is presented in the second.

Trapping Phenomena is another fascinating phenomenon of peristaltic motion. Essentially, it is the production of an internally circulating fluid gap utilizing a closed streamline. This captured gap propelled the head along peristaltic waves. (Figure 1-Figure 9) Describe the effect of the parameters $\boldsymbol{\Omega}, \boldsymbol{M}, \boldsymbol{Gr}, \boldsymbol{m}, \boldsymbol{A},\ \boldsymbol{\alpha}, \boldsymbol{B}, \boldsymbol{Da}, \boldsymbol{and}\ \boldsymbol{\phi}$ on stream function.

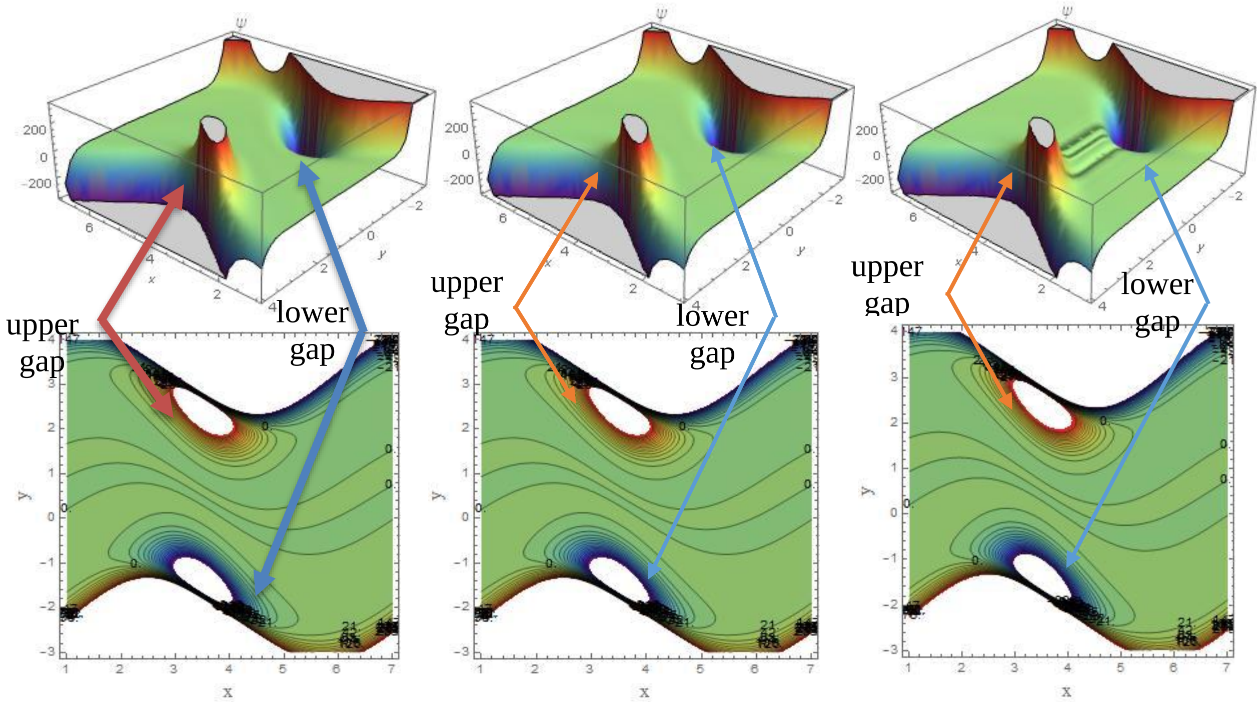

Figure 1. Distribution of streamlines for (a)**Ω**=1, (b)**Ω**=1.033, (c)**Ω**=1.066, $\boldsymbol{M=0.99}$, $\mathbf{Gr=0.5}$, $\boldsymbol{m=0.05}$, $\boldsymbol{A=3}$, $\boldsymbol{\alpha=2.5}$, $\boldsymbol{B=1}$, $\mathbf{Da=6}$, $\boldsymbol{\phi=2.4}$, $\boldsymbol{\rho=1}$, $\boldsymbol{d=1}$, $\boldsymbol{\mu=1}$, $\boldsymbol{a=0.8}$, $\boldsymbol{b=0.8}$, $\boldsymbol{d_1=0.001}$, $\boldsymbol{F_0=0.01}$, $\boldsymbol{\beta_1=0.05}$
(1) In 2 dimensions (2) In 3 dimensions.

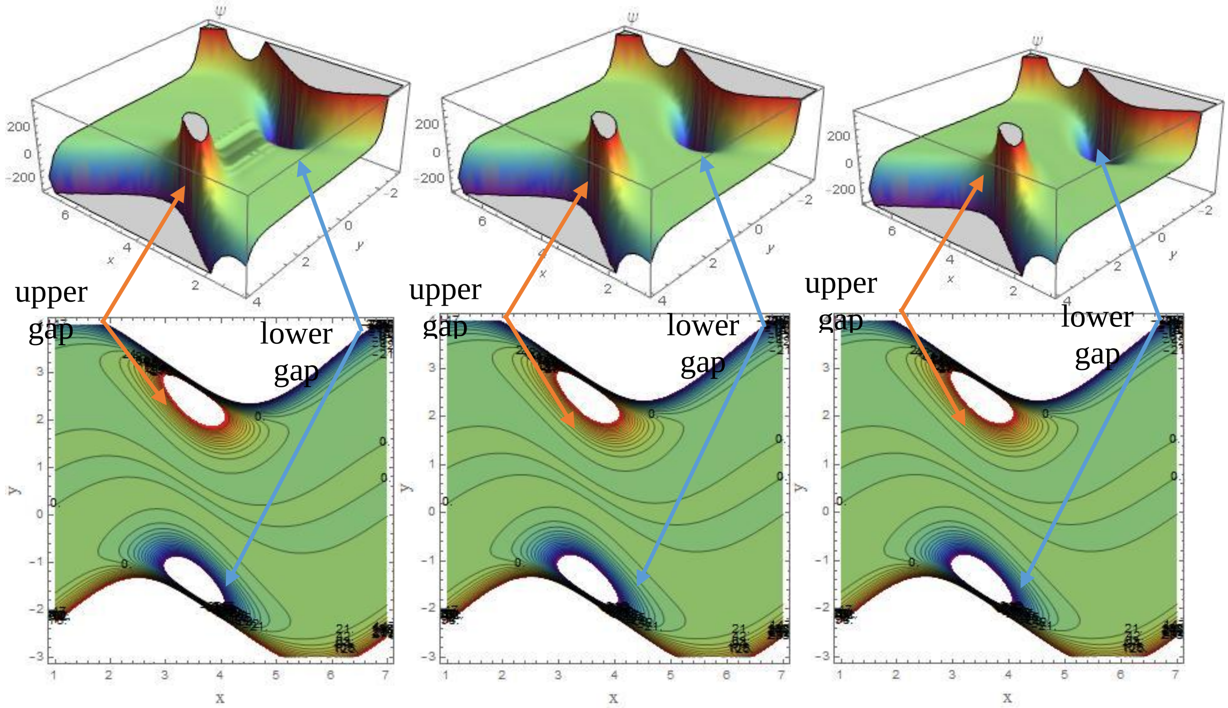

Figure 2. Distribution of streamlines for $\Omega=1$, (a)M=0.92,(b)$M = 0.95, (c)M = 0.99$, Gr $= 0.5, m = 0.05, A = 3, \alpha = 2.5, B = 1$, Da $= 6, \phi = 2.4, \rho = 1, d = 1, \mu = 1, a = 0.8, b = 0.8, d_1 = 0.001,\ F_0 = 0.01, \beta_1 = 0.05$
(1) In 2 dimensions (2) In 3 dimensions

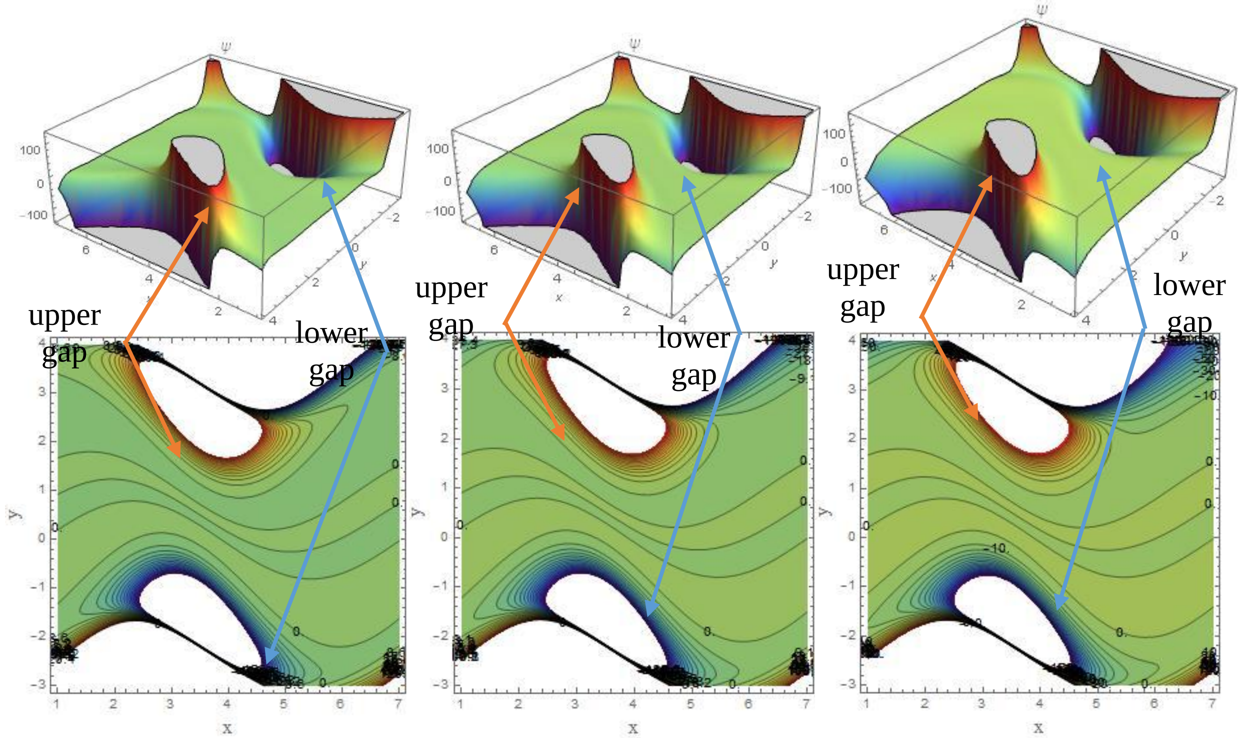

Figure 3. Distribution of streamlines for $\Omega=1$, $M = 0.99, (a)Gr = 1, (b)Gr = 5, (c)$Gr $= 10, m = 0.05, A = 3, \alpha = 2.5, B = 1$, Da $= 6, \phi = 2.4, \rho = 1, d = 1, \mu = 1, a = 0.8, b = 0.8, d_1 = 0.001, F_0 = 0.01, \beta_1 = 0.05$
(1) In 2 dimensions (2) In 3 dimensions..

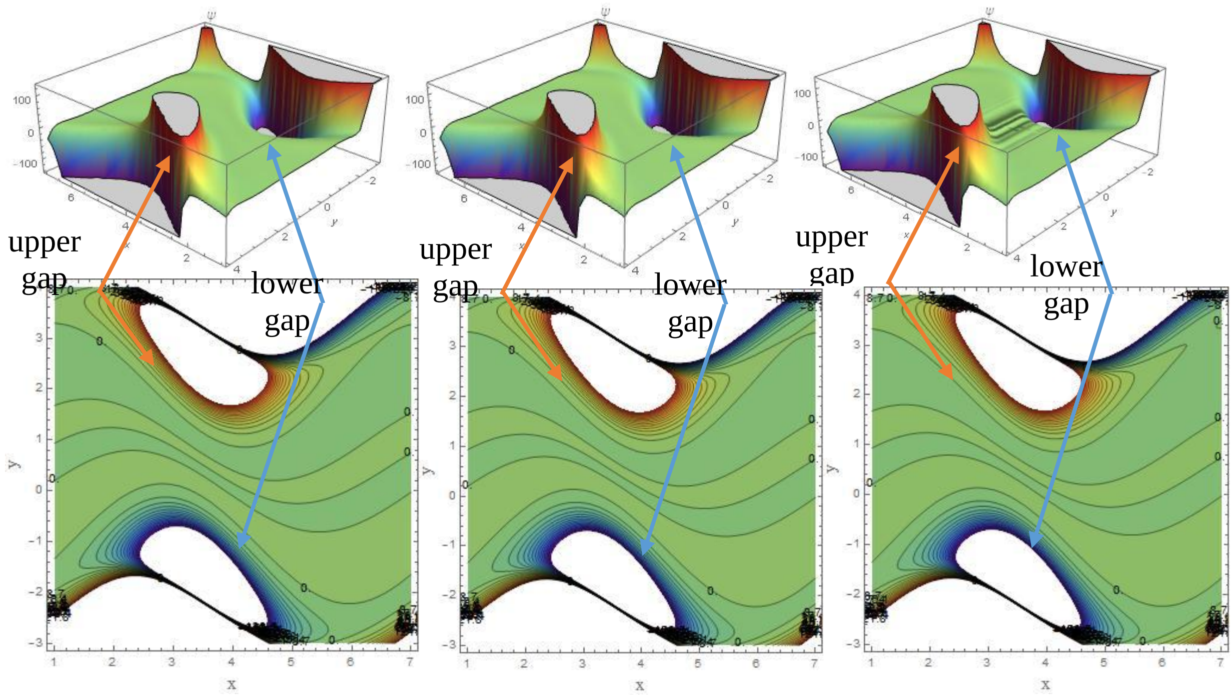

Figure 4. Distribution of streamlines for Ω=1, $M = 0.99, Gr = 0.5, (a) m = 0.05, (b) m = 0.2, (c) m = 0.4, A = 3, \alpha = 2.5, B = 1, Da = 6, \phi = 2.4, \rho = 1, d = 1, \mu = 1, a = 0.8, b = 0.8, d_1 = 0.001, F_0 = 0.01, \beta_1 = 0.05$
(1) In 2 dimensions (2) In 3 dimensions

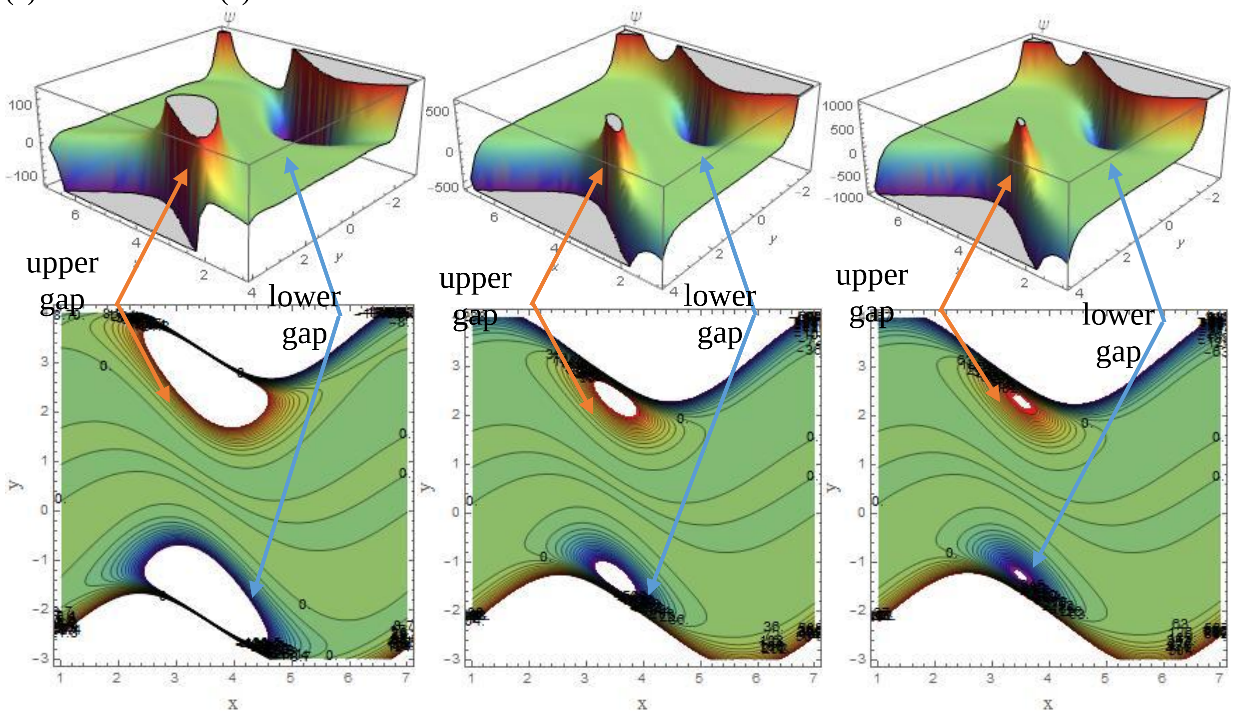

Figure 5. Distribution of streamlines for Ω=1, $M = 0.99, \mathrm{Gr} = 0.5, m = 0.05, (a) A = 1, (b) A = 5, (c) A = 9, \alpha = 2.5, B = 1, \mathrm{Da} = 6, \phi = 2.4, \rho = 1, d = 1, \mu = 1, a = 0.8, b = 0.8, d_1 = 0.001, F_0 = 0.01, \beta_1 = 0.05$
(1) In 2 dimensions (2) In 3 dimensions

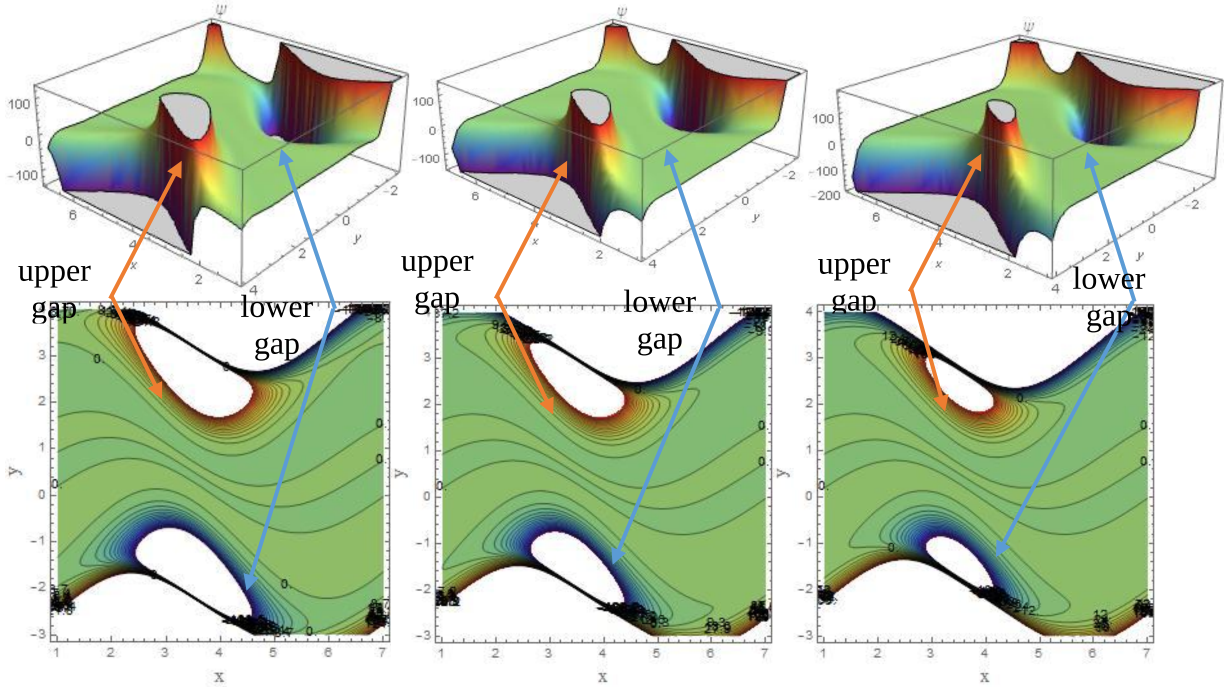

Figure 6. Distribution of streamlines for $\Omega=1$, $M = 0.99, Gr = 0.5, m = 0.05, A = 3, (a)\alpha = 2.5, (b)\alpha = 2.75, (c)\alpha = 3, B = 1, Da = 6, \phi = 2.4, \rho = 1, d = 1, \mu = 1, a = 0.8, b = 0.8, d_1 = 0.001,\ F_0 = 0.01, \beta_1 = 0.05$
(1) In 2 dimensions (2) In 3 dimensions

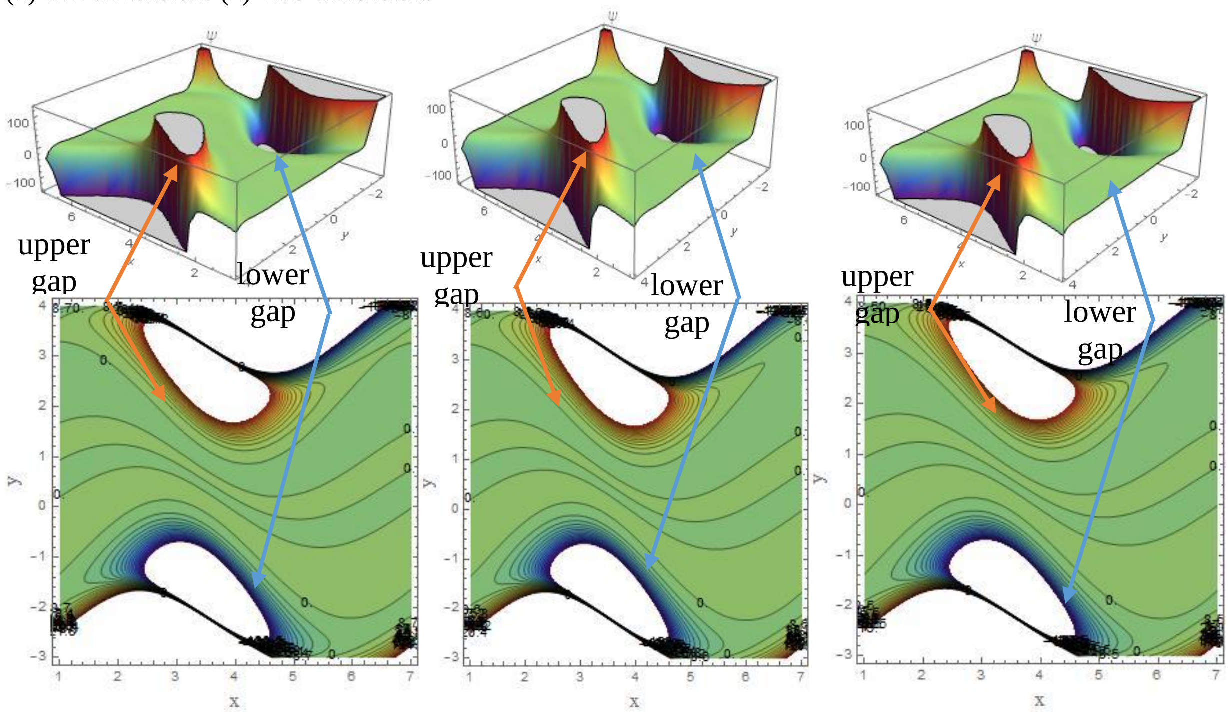

Figure 7. Distribution of streamlines for Ω=1, $\mathrm{M} = 0.99, \mathrm{Gr} = 0.5, \mathrm{m} = 0.05, \mathrm{A} = 3, \alpha = 2.5, (\mathrm{a})\mathrm{B} = 1, (\mathrm{b})\mathrm{B} = 2, (\mathrm{c})\mathrm{B} = 3, \mathrm{Da} = 6, \phi = 2.4, \rho = 1, \mathrm{d} = 1, \mu = 1, \mathrm{a} = 0.8, \mathrm{b} = 0.8, \mathrm{d}_1 = 0.001,\ \mathrm{F}_0 = 0.01, \beta_1 = 0.05$
(1) In 2 dimensions (2) In 3 dimensions.

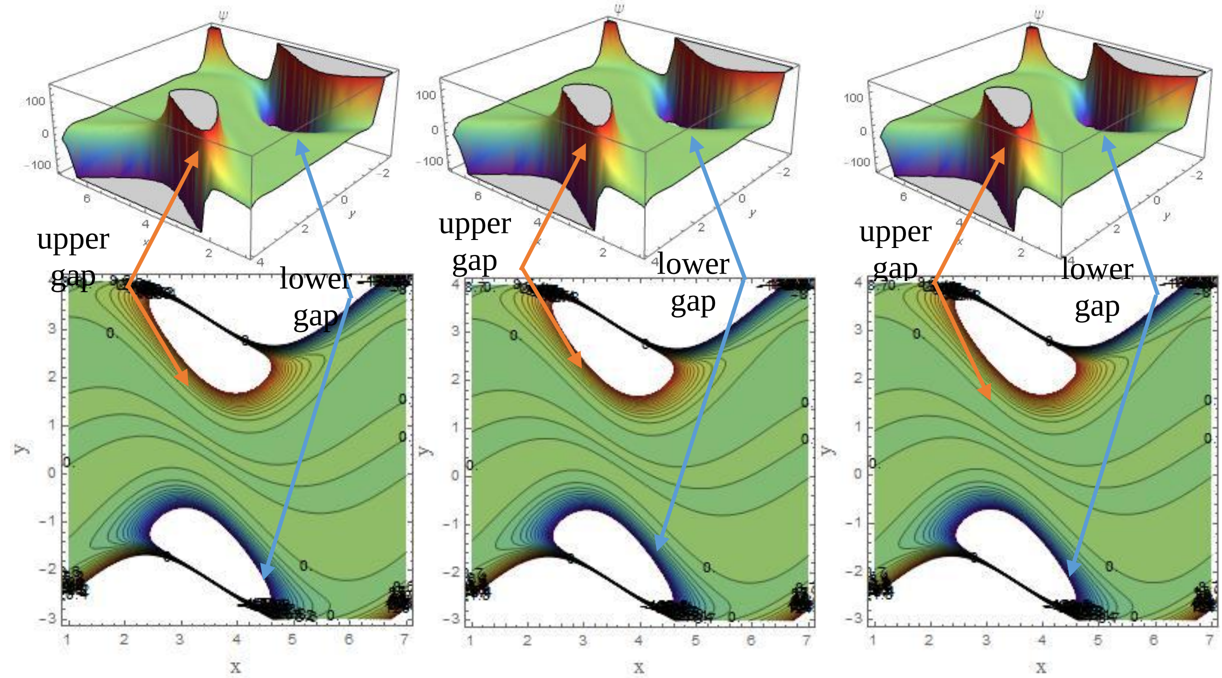

Figure 8. Distribution of streamlines for $\Omega=1$, $M = 0.99, Gr = 0.5, m = 0.05, A = 3, \alpha = 2.5, B = 1,$ (a)$Da = 3, (b) Da = 6, (c) Da = 9, \phi = 2.4, \rho = 1, d = 1, \mu = 1, a = 0.8, b = 0.8, d_1 = 0.001,\ F_0 = 0.01, \beta_1 = 0.05$
(1) In 2 dimensions (2) In 3 dimensions.

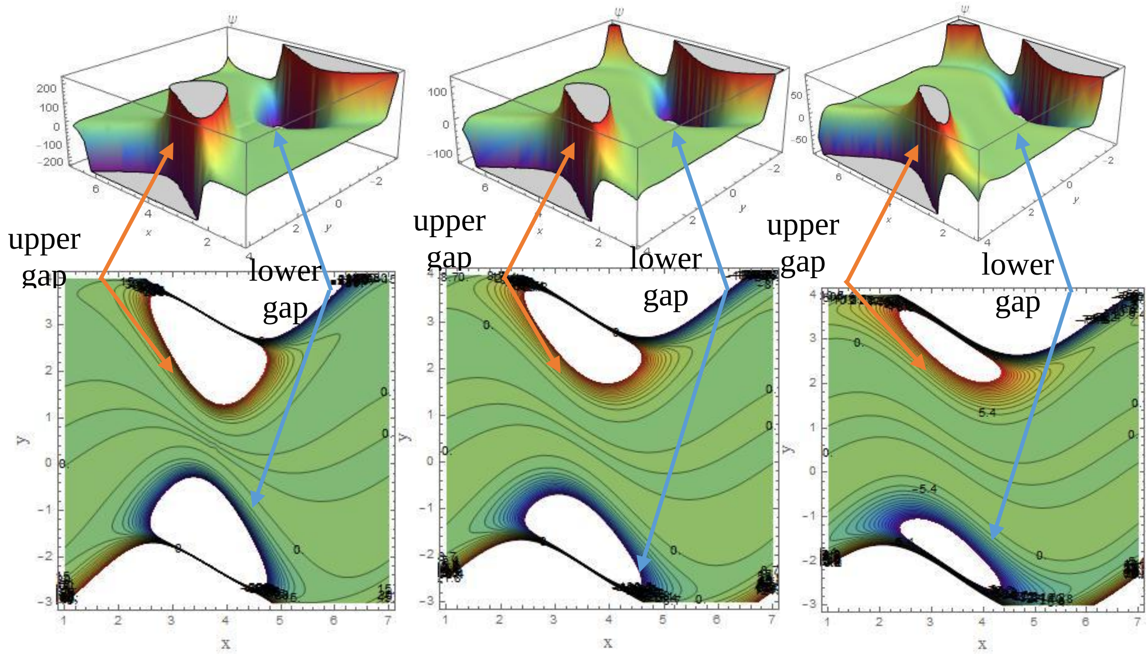

Figure 9. Distribution of streamlines for $\Omega=1$, $M = 0.99, Gr = 0.5, m = 0.05, A = 3, \alpha = 2.5, B = 1, Da = 6, (a) \phi = 2.1, (b) \phi = 2.4, (c) \phi = 2.7, \rho = 1, d = 1, \mu = 1, a = 0.8, b = 0.8, d_1 = 0.001,\ F_0 = 0.01, \beta_1 = 0.05$
(1) In 2 dimensions (2) In 3 dimensions.

4. Discussions

As show in result, the upper gap size and the lower gap size do not affect by an increase in the rotation (Ω). The upper gap size and the lower gap size do not affect by increasing the Hartmann number (M). With increasing the Thermal Grashof number (Gr), the size of the upper gap size and lower gap decreases. The size of the upper gap and lower gap have no effect by increasing Hall parameter (m). The size of the upper and lower gaps decreases with the increase of the fluid parameter (A). The upper gap size and the lower gap size don't change with increasing the couple stress parameter (α). The upper gap and lower gap slightly decreases with increasing the constant heat radiation (B). As the Darcy number (Da) goes up, the size of the upper gap and lower gap don't change. The size of the upper gap and lower gap decreases with the increase of the wavelength (ϕ).

5. Conclusions

In this article, the influence of heat transfer and rotation on a Sutterby fluid in an asymmetric channel was investigated. In this investigation, a lot of attention has been paid to the analysis of things like stream function based on a simple analytical solution. The key findings of the current research are summarized below:

- As (Ω), (M), (m), and (Da) goes up, the upper gap size and the lower gap size have no effect.
- As ($\boldsymbol{Gr}$), ($\boldsymbol{A}$), ($\boldsymbol{\alpha}$), and ($\boldsymbol{\phi}$) increase, The size of the upper gap and lower gap slightly decreases.
- As ($\boldsymbol{B}$) increases, The size of the upper gap and lower gap slightly decreases.

Acknowledgment

We hereby confirm that all the Figures and Tables in the manuscript are ours. Furthermore, any figures and images, that are not ours, have been included with the necessary permission for republication, which is attached to the manuscript.

Conflict of Interest

The authors declare that they have no conflicts of interest.

Ethical Clearance

The project was approved by the local ethical committee in University of Baghdad.

References

1. Mohaisen HN, Abedulhadi AM. Effects of the Rotation on the Mixed Convection Heat Transfer Analysis for the Peristaltic Transport of Viscoplastic Fluid in Asymmetric Channel. Iraqi J Sci. 2022;1240–57. https://doi.org/10.24996/ijs.2022.63.3.29
2. Hayat T, Ayub S, Alsaedi A, Tanveer A, Ahmad B. Numerical simulation for peristaltic activity of Sutterby fluid with modified Darcy's law. Results Phys. 2017;7:762–8. https://doi.org/10.24996/ijs.2022.63.3.29
3. Latham TW. Fluid motions in a peristaltic pump. Massachusetts Institute of Technology; 1966.
4. Shapiro AH, Jaffrin MY, Weinberg SL. Peristaltic pumping with long wavelengths at low Reynolds number. J Fluid Mech. 1969;37(4):799–825. https://doi.org/10.24996/ijs.2022.63.3.29
5. Kareem RS, Abdulhadi AM. Impacts of Heat and Mass Transfer on Magneto Hydrodynamic Peristaltic Flow Having Temperature-dependent Properties in an Inclined Channel Through Porous Media. Iraqi J Sci. 2020;854–69. https://doi.org/10.24996/ijs.2022.63.3.29
6. Ali HA. Impact of Varying Viscosity with Hall Current on Peristaltic Flow of Viscoelastic Fluid Through Porous Medium in Irregular Microchannel. Iraqi J Sci. 2022;1265–76. https://doi.org/10.24996/ijs.2022.63.3.29
7. Nassief AM, Murad MA. The influence of magnetohydrodynamic flow and slip condition on generalized Burgers' fluid with fractional derivative. Baghdad Sci J. 2020;17(1). https://doi.org/10.24996/ijs.2022.63.3.29
8. El-Dabe NTM, Moatimid GM, Mohamed MAA, Mohamed YM. A couple stress of peristaltic motion of Sutterby micropolar nanofluid inside a symmetric channel with a strong magnetic field and Hall currents effect. Arch Appl Mech. 2021;91(9):3987–4010. https://doi.org/10.24996/ijs.2022.63.3.29

9. Abdulhussein H, Abdulhadi AM. Impact of Couple Stress and Rotation on Peristaltic Transport of a Powell-Eyring Fluid in an Inclined Asymmetric Channel with Hall and Joule Heating Hanaa. J Basic Sci. 2022;8(13):483–509.
10. Hummady L, Abdulhadi A. Influence of MHD on peristaltic flow of couple stress fluid through a porous medium with slip effect. Adv Phys Theor Appl. 2014;30.
11. Abdulhadi AM, Ahmed TS. Effect of magnetic field on peristaltic flow of Walters' B fluid through a porous medium in a tapered asymmetric channel. J Adv Math. 2017;1(12):6889–93. https://doi.org/10.24297/jam.v12i12.4440
12. Sadaf H, Akbar MU, Nadeem S. Induced magnetic field analysis for the peristaltic transport of non-Newtonian nanofluid in an annulus. Math Comput Simul. 2018;148:16–36. https://doi.org/10.1016/j.matcom.2017.12.009
13. Salih AW, Habeeb SB. Influence Of Rotation, Variable Viscosity And Temperature On Peristaltic Transport In An Asymmetric Channel. Turkish J Comput Math Educ. 2021;12(6):1047–59.
14. Sutterby JL. Laminar converging flow of dilute polymer solutions in conical sections: Part I. Viscosity data, new viscosity model, tube flow solution. AIChE J. 1966;12(1):63–8. https://doi.org/10.1002/aic.690120114
15. Hayat T, Nisar Z, Alsaedi A, Ahmad B. Analysis of activation energy and entropy generation in mixed convective peristaltic transport of Sutterby nanofluid. J Therm Anal Calorim. 2021;143(3):1867–80.
16. Alshareef TS. Impress of rotation and an inclined MHD on waveform motion of the non-Newtonian fluid through porous canal. In: J Phys Conf Ser. IOP Publishing; 2020. p. 12061. https://doi.org/10.1088/1742-6596/1591/1/012061
17. Kalyani K, MVVNL SR. A Numerical Study on Cross Diffusion Cattaneo-Christov Impacts of MHD Micropolar Fluid Across a Paraboloid. Iraqi J Sci. 2021;1238–64. https://doi.org/10.24996/ijs.2021.62.4.20
18. Khudair WS, Dwail HH. Studying the magnetohydrodynamics for williamson fluid with varying temperature and concentration in an inclined channel with variable viscosity. Baghdad Sci J. 2021;18(3). https://doi.org/10.21123/bsj.2021.18.3.0531
19. Ahmad S, Farooq M, Javed M, Anjum A. Double stratification effects in chemically reactive squeezed Sutterby fluid flow with thermal radiation and mixed convection. Results Phys. 2018;8:1250–9. https://doi.org/10.1016/j.rinp.2018.01.043
20. Ramesh K, Prakash J. Thermal analysis for heat transfer enhancement in electroosmosis-modulated peristaltic transport of Sutterby nanofluids in a microfluidic vessel. J Therm Anal Calorim. 2019;138(2):1311–26. https://doi.org/10.1007/s10973-018-7939-7
21. Atlas F, Javed M, Imran N. Effects of heat and mass transfer on the peristaltic motion of Sutterby fluid in an inclined channel. Multidiscip Model Mater Struct. 2020;16(6):1357–72. https://doi.org/10.1108/MMMS-08-2019-0156
22. Abdulla SA, Hummady LZ. Inclined magnetic field and heat transfer of asymmetric and porous medium channel on hyperbolic tangent peristaltic flow. Int J Nonlinear Anal Appl. 2021;12(2):2359–73. https://doi.org/10.22075/IJNAA.2021.5382